The influence of the oxygen reduction reaction (ORR) on Pt oxide electrochemistry

Oliver Rodríguez[1,2] and Guy Denuault*[1]

[1]Chemistry, University of Southampton, Southampton, SO17 1BJ, UK.

[2]Current address: Beckman Institute for Advance Science and Technology, University of Illinois at Urbana-Champaign, Urbana 61801, USA.

*Corresponding author

*E-mail: gd@soton.ac.uk

Dedicated to Prof. Marcin Opallo on the occasion of his 65th birthday.

Abstract

In this study, we employed microelectrodes and scanning electrochemical microscopy (SECM) to investigate the role of molecular oxygen and local pH changes on the electrochemistry of Pt oxide. We show that in acidic media and alkaline conditions, the impact of O_2 is negligible, while in unbuffered neutral media, O_2 strongly affects the formation of Pt oxides. Experiments carried under hindered diffusion reveal that this is due to a high local pH arising from the oxygen reduction reaction. This is evidenced by the appearance, at very positive potentials, of a diffusion controlled wave consistent with the oxidation of OH^-. The ORR produces a sufficiently alkaline environment near the electrode to promote the formation of oxide at much more negative potentials than anticipated from the bulk pH. As a result, the onset of oxide formation overlaps the onset of oxygen reduction and it is impossible to obtain a Pt surface free from oxide at potentials positive of the onset of the ORR. Thus, prior exposure of the Pt surface to dissolved oxygen does not leave irreversibly adsorbed oxygen species as previously reported by our group; instead, the ORR induces a coverage of oxide at much lower potentials than determined by the bulk pH.

Keywords: oxygen reduction reaction, ORR, Pt oxide, pH effects, scanning electrochemical microscopy, SECM.

1 Introduction

Oxidized platinum surfaces can be detrimental for certain technologically important reactions such as the oxygen reduction and the hydrogen peroxide reduction [1, 2, 3], but surprisingly, few studies have considered the effect of dissolved oxygen on the electrochemistry of Pt oxide. Hoare's group [4, 5] investigated how dissolved oxygen interacted with the first few layers of the Pt lattice. Using X-ray diffraction, Drnec and co-workers [6] concluded that for Pt(111) in $HClO_4$, the ORR did not significantly influence the early stages of Pt oxide formation. Using on line mass spectrometry, Topalov and co-workers reported that oxygen did not interfere with the fundamental processes of surface oxidation/reduction [7]. Using flow cells to switch from an O_2 saturated solution to one without O_2, forming oxide in the presence of O_2 and stripping it in its absence, Kongkanand's and Liu's groups [8, 9] independently concluded that O_2 does not have an appreciable effect on oxide coverages. In contrast, Matsumoto and co-workers found that Pt dissolution was significantly enhanced while potential cycling in presence of dissolved oxygen [10]. Similarly, our group reported that oxygenated species found adsorbed on metallic microdisc electrodes were related to the presence of molecular oxygen in solution and that their adsorption was irreversible as they could be detected even after removing O_2 from solution [11, 12]. We also observed that their coverage depended on the oxygen concentration and on the affinity of the electrolyte anions for Pt; with the coverage of oxygenated species increasing with the bulk oxygen concentration and decreasing in the order ClO_4^-, Cl^-, Br^- and I^-. In presence of strongly binding anions such as I^-, no adsorbed oxygen species were observed. Even though all the experimental evidence pointed at O_2 being the source of the adspecies, their true nature and identity remained unknown. Apart from differences in the techniques used, the most important difference between our work and the other studies seemed to be the pH. The other works had been performed under acidic conditions, while ours had been carried out in unbuffered neutral media [11, 12, 13, 14, 15]. Changes in local pH during electrochemical reactions are often exploited to control deposition processes, e.g. sol-gel, polymers and nanoparticles [16, 17, 18, 19] but less often considered in electrocatalysis because most reactions are investigated in strongly acidic or alkaline media. With this in mind, we set out to study the influence of O_2 and pH on the adsorption of oxygenated species on Pt.

In the following, we first consider the impact of the bulk pH and of the gas used to saturate the solution (O_2 or Ar), then we show how using the hindered diffusion mode of the scanning electrochemical microscope helped us study the impact of local pH changes and unravel the role of dissolved oxygen on the formation of Pt oxides.

2 Experimental

Ar (99.999 %, BOC), O_2 (99.5 %, BOC), H_2SO_4 (95-98 %, Sigma-Aldrich), $HClO_4$ (99.999 %, Sigma-Aldrich), NaOH (97 %, Fisher Chemical), $KClO_4$ (99.99 %, Sigma-Aldrich), $KMnO_4$ (99.5 %, AnalR) and H_2O_2 (30 % w/v, Fisher Chemical) were used as received. Air was obtained from an external compressor.

The solutions were prepared with water from a Purite system (18 MΩ cm). Decision was taken to keep the solutions as simple as possible to avoid the impact of additional ions on the surface processes and the ORR. For this reason, no attempt was made to buffer the neutral solutions. All experiments were performed in a two-electrode arrangement with a PGSTAT101 potentiostat (Autolab), a Pt microdisc (ϕ = 50 μm, Goodfellow) as the working electrode and a reversible hydrogen electrode (Gaskatel) as counter-reference electrode. The Pt microdisc was sealed in glass ($RG = 50$ where RG is the radius of the glass sheath divided by the disc radius a), polished with emery paper (600 and 1200 grit) and alumina suspension (5, 1 and 0.3 μm, MetPrep). Conventional experiments were conducted in a thermostated (25 ^{o}C) five-neck glass jacketed-cell placed inside a grounded Faraday cage. Ar, O_2 or air were passed through a Dreschell bottle filled with water to humidify them and trap particles before being introduced into the solutions. During the experiments, the gas was kept flowing above the solution and the cell outlet was connected to a water trap to prevent ambient air from entering the cell. Before use, all the glassware was soaked overnight in a solution consisting of 0.7 g/L of $KMnO_4$ with 40 mM H_2SO_4 followed by soaking for several hours in a diluted piranha solution (30 mM H_2O_2 and 40 mM H_2SO_4) to remove organic residues; beware, this very corrosive solution causes severe chemical burns. The glassware was then boiled in deionised water three times for 30 min each. After the cleaning procedure, all the glassware was kept in deionised water to minimise the chance of contamination. SECM experiments involved an open home-made glass cell. The cross section of a glass rod (ϕ = 7 mm) was polished with emery paper (600 then 1200 grit) and alumina (5, 1 and 0.3 μm) and used as an inert substrate to operate under hindered diffusion (SECM negative feedback). The SECM tip, a Pt disc (ϕ = 50 μm) set in glass ($RG = 50$) was held by a 3-axis micropositioner (three M-605 high precision linear stages, PI-Instruments). The tip was carefully positioned parallel to the substrate and the tip-substrate distance was determined by fiting the experimental approach curve to the theoretical expression [20]. Voltammetric experiments were typically carried out at 200 or 500 mV s^{-1} because these scan rates are sufficiently large to reveal the Faradaic response from adsorbed species but sufficiently small to retain the diffusion controlled sigmoidal wave for the ORR on the microdisc. This approach ensures that the voltammograms present the contribution from all Faradaic processes.

3 Results

3.1 Experiments in the bulk

In this section, we present the voltammograms recorded with the microdisc electrode in bulk solutions with and without dissolved oxygen. Three solutions were considered, 0.1 M $HClO_4$, 0.1 M $KClO_4$ and 0.1 M NaOH. Voltammograms for the first two are presented here while those for the alkaline conditions are in supplementary information.

In 0.1 M $HClO_4$, Figure 1a, the Pt microdisc produces voltammograms typical for a Pt electrode in acidic media. Figure 1b shows the same results but on a more sensitive scale to highlight the Pt oxide

region. In absence of oxygen, the voltammogram presents the well-known characteristics of polycrystalline Pt surface reactions [21]. In presence of oxygen, the oxide region is unaffected until the ORR begins. The ORR wave starts at potentials well into the oxide formation region, circa 1 V for the anodic sweep and 0.8 V for the cathodic one. This discrepancy has been related to the state of the surface. On the cathodic sweep, the electrode is covered by oxygen species, presumably PtOH [21, 22, 23, 24, 25], and the ORR onset potential is reported to depend on its coverage [1, 2, 3, 26]. On steady state voltammograms, these effects are clearly evidenced by a hysteresis between the cathodic and anodic sweeps, coupled with two crossover points; see also the supporting information from Ref. [12]. Here, the hysteresis is also enhanced by transient diffusion since the sweep rate is too large for the microelectrode to operate under steady state conditions [27]. Similar observations can be made for the voltammograms recorded in NaOH, Figure S1 in supplementary information. In this medium, the ORR onset is still located in the oxide formation region, circa 1 V, and two crossover points are clearly visible but the hysteresis is much less pronounced.

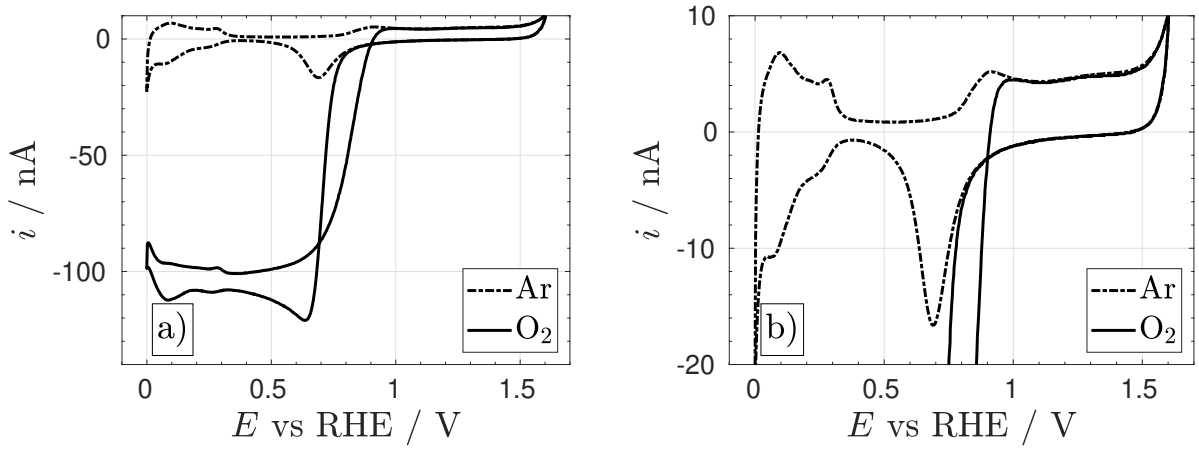

Figure 1: a) Cyclic voltammograms (15th cycle) recorded at 200 mV s^{-1} with a Pt disc electrode (ϕ = 50 μm) in Ar and O_2 saturated 0.1 M $HClO_4$ solution. b) same as in a) but focusing on the Ar saturated CV.

In $KClO_4$, Figure 2, the voltammetry is altered. In absence of oxygen, the voltammogram presents significant differences compared to those recorded in acidic and alkaline conditions. The most prominent are the irreversibility of the hydrogen adsorption-desorption processes and the fact that the onset of hydrogen evolution is not located at 0 V on the RHE scale. Similar observations in neutral unbuffered media have been attributed to local pH changes due to the inability of the solution to maintain the bulk pH close to the electrode surface [21, 28]. This situation arises because all the Faradaic surface processes consume H^+ (alternatively produce OH^-) during the cathodic sweep and consume OH^- (alternatively produce H^+) during the anodic sweep. Thus, the OH^- ions left behind during oxide reduction and hydrogen adsorption, make the electrode environment more alkaline. The reference electrode relies on the bulk pH to pin the potential scale; it cannot compensate for pH changes near the working electrode and the corresponding voltammetric

features, including the onset of hydrogen evolution, occur at more negative potentials. Similarly, the H^+ ions released during hydrogen desorption and oxide formation acidify the local solution, and the corresponding voltammetric features appear at more positive potentials. In absence of buffer, or in weakly buffering solutions, any surface reaction involving H^+ and OH^- impacts on the subsequent reaction during the potential sweep. This situation is further complicated by the mass transport conditions. Low rates of mass transport allow H^+ and OH^- ions to linger close to the electrode while high rates of mass transport rapidly re-adjust the local pH to its bulk value [13, 21, 28]. Furthermore, high rates of mass transport, as found with a microdisc electrode, help reveal kinetic limitations. For adsorbed redox species, this translates in a shift of the oxidation peak towards positive potentials and a shift of the reduction peak towards negative potentials. In the bulk experiments discussed here, the rate of mass transport was not varied (same sweep rate and same electrode radius throughout) to simplify the interpretation of the voltammetry so the analysis is entirely based on the role of the pH near the electrode surface. Interestingly, in presence of oxygen, there was no voltammetric evidence of gradual alkalinisation of the solution near the electrode from one cycle to the next; the CV only required two cycles to stabilise in presence of oxygen but over ten in absence of oxygen. This is the reason why we present the 15^{th} cycle.

For the hydrogen region, the variations in local pH have a dramatic effect. Where the adsorption and desorption peaks occur at the same potential in acidic and alkaline media, they are separated by circa 430 mV in 0.1 M $KClO_4$. The impact of the local pH on the oxide formation region is more difficult to assess due to the number of processes involved. Briefly, Pt oxidation is reported to involve the physisorption of water molecules, the formation of PtOH, the increase in PtOH coverage with potential until the place exchange mechanism takes place, around 1.1 to 1.2 V [25], and eventually, multilayer formation [2, 25, 26, 29]. These processes release H^+ and acidify the electrode environment, thereby shifting the subsequent voltammetric peaks towards more positive potentials. In summary, in neutral unbuffered media, the variations in local pH due to the surface reactions and the influence of mass transport, produce a much more complex Pt voltammogram than in acidic or basic media. We now consider the role of oxygen and discuss how it affects the voltammetry of Pt in a neutral unbuffered solution.

When 0.1 M $KClO_4$ is saturated with oxygen, the Pt voltammetry is even more affected. The hydrogen region, Figure 2a, is still at more negative potentials than anticipated from the bulk pH but it appears far more reversible than in absence of oxygen. Similar observations were made in comparable conditions with stationary Pt macroelectrodes [28]. The oxide formation region, Figure 2b, is also affected by the presence of O_2. The first oxide formation peak appears at more negative potentials than in absence of O_2. Then, the current drops to a minimum before rising to form an oxidation wave at roughly the same potential as the second oxide formation peak seen in absence of oxygen. On the reverse sweep, the oxide reduction peak occurs at more negative potentials than in absence of oxygen. To interpret these observations we once again consider the impact of local pH changes, however, this time, we take into account the influence of the ORR. Since the rate of OH^- production is linked to the ORR rate and therefore to the rate of mass transport,

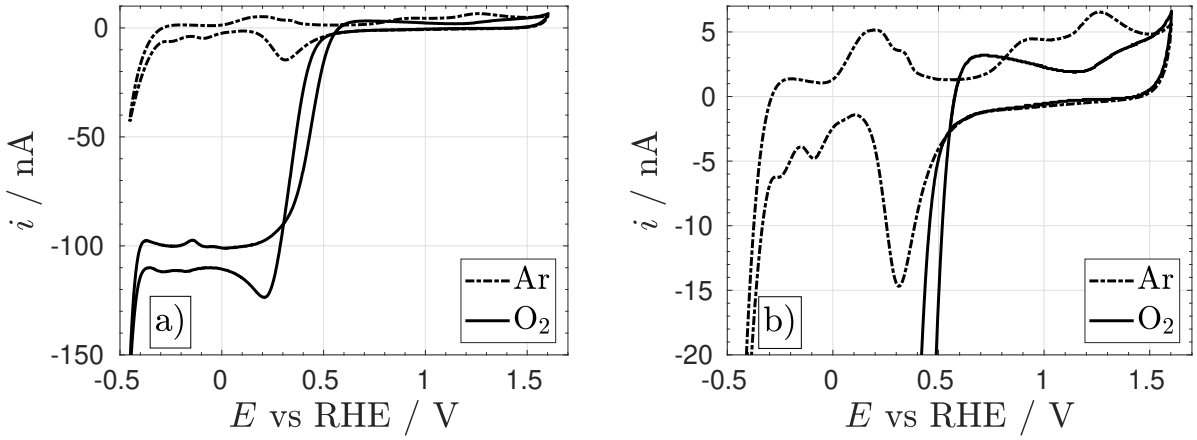

Figure 2: a) Cyclic voltammograms (15th cycle) recorded at 200 mV s^{-1} in Ar and O_2 saturated 0.1 M $KClO_4$ solution with a Pt disc electrode ($\phi = 50$ μm). b) same as a) but focusing on the Ar saturated CV.

it is not possible to prevent significant changes in local pH without addition of a strong buffer. In strong acidic, Figure 1, and alkaline, Figure S1, solutions, the ORR is not able to influence the local pH and the voltammetric features of Pt appear at potentials dictated by the bulk pH (see also reference [30] for examples of CVs in neutral and buffered media).

Based on the above discussion, we can interpret the voltammetry shown in Figure 2 as follows. At the start of the ORR, circa 0.6 V, the reaction begins to produce OH^- and this shifts the Pt oxide reduction peak circa 100 mV more negative than in absence of oxygen. This suggests that the local pH has increased by circa 1.7 units. Moving towards negative potentials, the ORR continually produces a high flux of OH^-. Even with the high rate of mass transport at the microelectrode, the amount of OH^- left near the electrode is sufficient to force the hydrogen adsorption to occur under strong alkaline conditions. For the same reason, the onset of hydrogen evolution occurs at more negative potentials than in absence of oxygen. During the reverse sweep towards positive potentials, the ORR continues to produce OH^- and the desorption of hydrogen occurs in similarly alkaline conditions. As a result, the hydrogen region appears far more reversible than in Ar-saturated conditions. The ORR rate drops as we move further on towards positive potentials but there is still enough OH^- left near the electrode to promote oxide formation at more negative potentials than expected from the bulk pH, in fact at potentials close to those observed in alkaline conditions. The first peak corresponding to oxide formation has shifted by approximately -240 mV, which suggests that at this point in the cycle, the local pH has increased by circa 4 units. At around 1.2 V, the solution near the electrode is now acidic, either because most OH^- ions have been taken away by mass transport (as the ORR does not occur in this region) or neutralised by the H^+ produced during the early stages of oxide formation. As a result, the next phase of oxide formation appears as a wave around the same potential as the second oxide formation peak seen in absence of oxygen. The switch from alkaline to acidic environment appears to

be the cause of the current minimum circa 1.2 V. This value is interesting because Perry and Denuault had observed that oxygen adspecies appeared in presence of dissolved oxygen when resting at potentials below 1.2 V while above this value, the rest potential led to oxide growth [11].

The results presented in Figure 2 therefore suggest that the local pH change induced by the ORR is the source of the adsorbed oxygen species reported by Perry and Denuault. In their work, they were able to observe the oxygen adspecies even after decreasing the bulk concentration of O_2, which suggests that even at a low OH^- production rate, the mass transport rate at the microelectrode was not high enough to compensate for the local change of pH. In the next section, we take a different approach, based on the concept of hindered diffusion, to investigate how the ORR influences the oxide formation region. Instead of increasing the mass transfer coefficient, we confine any OH^- formed between the microelectrode and an inert surface, and we observe how the resulting increase in the local pH affects the potentials of the Pt surface processes.

3.2 Hindered diffusion

Perry and Denuault reported that the potential needed to reduce the adspecies correlated well with the ORR potential window, and this led them to suggest that the adspecies was oxygenated in nature [11, 12]. As it only appeared when O_2 was present in solution, it proved difficult to study amperometrically without the contribution from the ORR current. To circumvent this problem, they employed a two stage procedure consisting of an adsorption step in the oxygenated electrolyte followed by a stripping step after deaerating the electrolyte [12], an approach similar to that used by Kongkanand and Liu [8, 9]. However, this protocol is not ideal because, as discussed above, the local pH is very different depending on the presence or absence of oxygen and the electrode effectively operates in two different environments. To avoid this issue, we followed a methodology that did not rely on changing or deaerating the solution. Instead, we worked under aerated conditions at all times and exploited the concept of SECM hindered diffusion to minimize the flux of O_2 towards the electrode. Although hindered diffusion of dissolved oxygen has been used in SECM to determine the tip-substrate distance without the need for a redox mediator [31], the idea of exploiting the hindered diffusion of oxygen to control its impact on the electrode voltammetry and on the local pH has, to our knowledge, never been reported previously. In SECM, hindered diffusion (a.k.a. negative feedback in SECM terminology) is achieved by approaching the tip of a microdisc electrode close to an inert substrate while holding the tip potential at a constant value to oxidise or reduce a redox species of interest under steady state conditions. When the tip-substrate distance is less than ten times the tip radius, the diffusion field of the redox species becomes blocked by the substrate and the tip current decreases with the tip-substrate distance. This arrangement is analogous to a leaky thin layer cell [32]. The hindrance also increases with the RG, the ratio between the insulating sheath radius and the microdisc radius [33]. In the following discussion, we call "bulk" a position where $L > 30$ and "hindered" one where $L < 5$, where $L = d/a$, with d the tip-substrate distance and a the microelectrode radius. The corresponding experimental and theoretical [33] approach

curves are presented in supplementary information.

Hindered diffusion offers several advantages: 1-the solution remains aerated and does not need to be changed, 2-O_2 is still present so the ORR can still occur, 3-the OH^- ions produced by the ORR are trapped in the thin electrolyte layer thus the local pH remains alkaline while the ORR is running, 4-the ORR current contribution is minimised and surface processes dominate the amperometric response, 5-it is possible to control the O_2 flux by changing the distance between the microelectrode and the inert substrate, 6-it is possible to move away from the substrate and record a reference voltammogram in the bulk of the solution, 7-it is possible to condition the electrode in the bulk, e.g. allow the oxygenated species to adsorb on the electrode, and perform a stripping analysis close to the inert substrate where the oxygen flux is minimised. Fast voltammetry could also be used to enhance the amperometric response of surface-bound species over that of diffusion controlled species but this technique has two drawbacks: it enhances the contribution of non-faradaic process such as the double layer charging, although this is less of an issue with microdisc electrodes, and it increases the rate of oxygen diffusion towards the electrode above that encountered in the steady state bulk conditions. In contrast, hindered diffusion offers a range of oxygen diffusion rates below that found in the steady state bulk conditions. It is also possible to change the rate of oxygen transport by exploiting microdisc electrodes with different radii but this approach does not offer the advantages of hindered diffusion listed above, furthermore, it requires a different microdisc for each diffusion rate and does not allow oxygen diffusion rates below that obtained in the steady state. In the following, we present the voltammetry recorded with the microelectrode and analyse the impact of the ORR in different pH for different tip substrate distances.

Figure 3a presents typical voltammograms recorded at the bulk ($L > 30$) and hindered ($L < 5$) positions in air-saturated 1 M H_2SO_4. A sweep rate of 500 mV s^{-1} was selected to reveal the amperometric response of the surface processes. In the bulk, the curve presents the characteristic voltammetry of Pt in acid but the double layer and hydrogen regions are vertically offset due to the ORR current. The oxygen reduction current is circa five times smaller than in Figure 1a because here the solution is only aerated. Close to the inert substrate, the hindered CV shows the same voltammetric features but with a much smaller vertical offset indicating that the ORR is still happening. O_2 is still able to diffuse from the bulk, but with a much lower flux because of the hindrance from the substrate and the insulating sheath around the tip. Interestingly, the hindered CV shows that the oxide formation region is unaffected by the remaining flux of O_2, and shows no evidence of local pH effects; this is presumably due to the high H^+ concentration that neutralises any OH^- formed during the ORR. Figure 3a therefore suggests that, in acidic conditions, hindering is equivalent to partial degassing provided the tip is approached sufficiently close to the inert substrate. This is not specific to oxygen reduction and the same approach could be exploited to investigate the amperometry of surface processes when redox species present in solution contribute to the total current.

In unbuffered neutral conditions, Figure 3b, the hindered CV shows the decreased ORR current expected from the lower flux of O_2; compared to that recorded in the bulk, the hydrogen region is unchanged but

there are clear differences in the oxide region; these are considered later on in this section. However, the hindered CV also presents differences with that recorded in the bulk in absence of oxygen, Figure 2. There, the hydrogen desorption region shifted positively by over 400 mV compared to the adsorption region; under hindrance, the hydrogen region only shifted positively by circa 200 mV. Interestingly, the same shift is observed when the CV is recorded in the bulk in presence of oxygen, so lowering the rate of oxygen diffusion does not affect the shift. Accounting for the ORR stoichiometry, the flux of OH^- away from the electrode is four times larger than the flux of oxygen reaching the electrode. Even accounting for the diffusion coefficient of OH^- [34] being almost twice larger than that of oxygen [15], there is still an accumulation of OH^- near the electrode, even at very low L values when the oxygen flux is hindered. Unbuffered neutral solutions are generally acidified by the solubility of CO_2 from the air but here we note that the oxide region recorded in the aerated bulk, Figure 3b, is identical to that recorded in the oxygen saturated bulk, Figure 2b, so the presence of dissolved CO_2 in the aerated solution did not appear to influence the voltammetry of the Pt oxide; for this reason, we did not consider the role of CO_2 further.

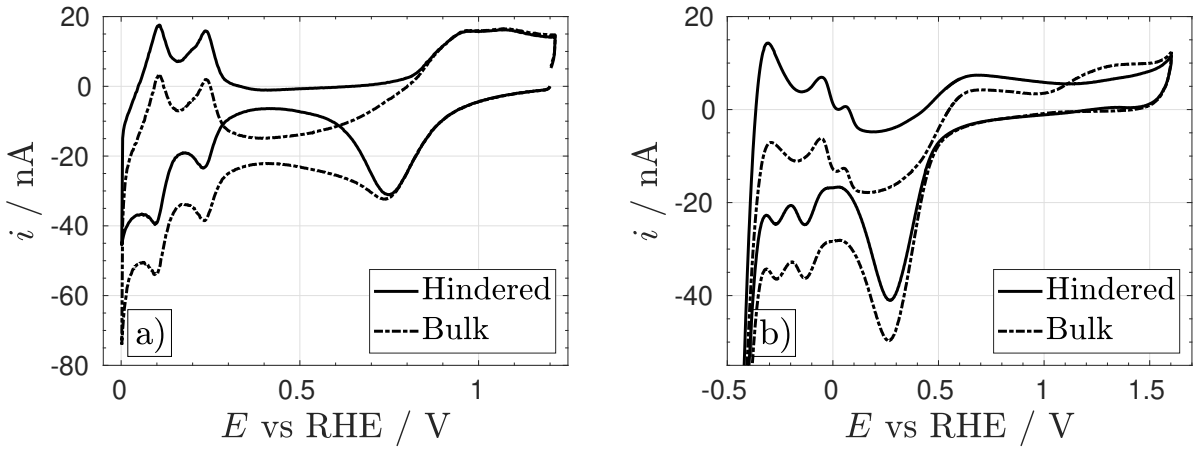

Figure 3: Cyclic voltammograms (1st cycle) recorded with a Pt disc electrode ($\phi = 50$ μm, $RG = 50$) at 500 mV s^{-1} in air saturated solutions, a) 1 M H_2SO_4, and b) 0.1 M $KClO_4$ in the bulk and hindered positions.

Recording the voltammogram at low scan rate, Figure 4, reveals an interesting phenomenon, the appearance of a new oxidation wave at potentials above 1.3 V; the complete CV is shown in supporting information. The currents are small because of the low scan rate but the hindrance has a clear influence on the oxide region. In the bulk, the oxide formation occurs in two clear stages as shown in Figure 2b with a ten time larger sweep rate. In contrast, the voltammogram recorded under hindrance shows an increased current for the first stage. This current is almost steady until around 1.3 V after which a clear oxidation wave is observed. In the cathodic sweep, the wave does not return immediately to zero current, as observed in the bulk or with acidic and alkaline conditions. Moreover, its sigmoidal shape is consistent with a steady state diffusion controlled process at a microdisc electrode. We believe that this wave reflects the oxidation of

OH^-, as it is known to occur on metallic microelectrodes at high potentials [35, 36, 37]. If this hypothesis is correct, the wave confirms that, despite the low rate of oxygen transport used here, the hydroxide ions from the ORR are concentrated in the thin layer of solution thereby making the local pH far more alkaline than in the bulk.

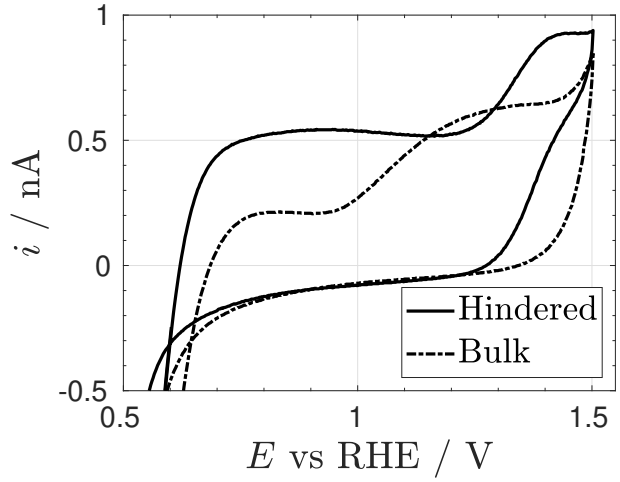

Figure 4: Cyclic voltammograms (2nd cycle) recorded with a Pt disc electrode ($\phi = 50$ μm, $RG = 50$) at 20 mV s^{-1} in an air saturated 0.1 M $KClO_4$ solution in the bulk and hindered positions.

If the extra wave seen in the hindered position is indeed related to the diffusion controlled oxidation of OH^-, then it should be possible to control its magnitude by varying the local pH. An increase in production of OH^- should increase the limiting current observed above 1.3 V, while the production of H^+ should decrease it. In addition, the local pH should be sensitive to the tip-substrate distance and the limiting current should change accordingly. To test this hypothesis, a potential waveform was designed to drive the oxygen reduction reaction and analyse the amount of OH^- produced by oxidation at positive potentials, Figure 5a. First, the potential was swept at 20 mV s^{-1} from 0.8 V to 0 V; a sweep was selected to allow visualisation of the corresponding current-potential response in real time, and its limits were selected to minimise oxide formation and prevent hydrogen adsorption respectively. Then the potential was held at $E_{low} = 0$ V for a certain amount of time t_{low}; this corresponds to the diffusion controlled reduction of O_2 where the rate of OH^- production is maximised. The sweep and the potential hold generate OH^- while t_{low} serves to control the amount of OH^- produced. After t_{low}, the potential was swept towards the oxidation region to detect OH^-; the potential was then swept back to E_{low} to finish the cycle. Voltammograms of the oxide formation region obtained for different values of t_{low}, Figure 5b, reveal that the limiting current of the oxidation wave seen above 1.3 V increases with t_{low}, thereby confirming that the oxidation wave is directly related to the ORR. Interestingly, the limiting current does not increase significantly when t_{low} approaches 300 s, a duration commensurate with the time needed for OH^- species to diffuse from the centre of the disc to the outer edge of the insulating sheath ($(RGa)^2/D = 347$ s with $RG = 50$, $a = 25$ μm and $D = 4.5\text{x}10^{-5}$ cm^2

s^{-1} [34]). These results are therefore consistent with the wave corresponding to the oxidation of the OH^- ions produced by the ORR with a maximum limiting current determined by the time needed for the ions to diffuse to the outer edge of the microelectrode. In future, a quantitative analysis of such experiments could be undertaken by numerically modelling the local pH taking into account the overall ORR stoichiometry, the diffusion of O_2 towards the tip, and the diffusion of OH^- away from the tip.

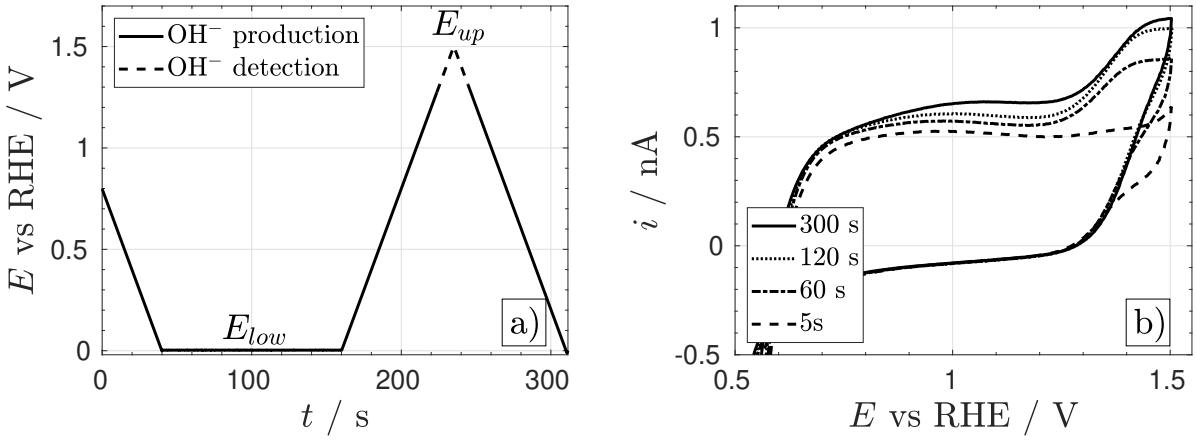

Figure 5: a) Potential waveform used to generate and detect OH^-, b) cyclic voltammograms recorded with a Pt disc electrode ($\phi = 50$ μm, $RG = 50$) at 20 mV s^{-1} in aerated 0.1 M $KClO_4$. The electrode was in the hindered position, $E_{low} = 0$ V and t_{low} was varied as indicated in the legend.

To continue testing the pH sensitivity of the oxidation wave, the upper potential of the waveform, E_{up}, was increased to reach the oxygen evolution reaction. The latter is known to produce H^+ in neutral conditions and H_2O in alkaline conditions; in both cases, OH^- is consumed, effectively lowering the local pH. Figure 6 shows the results for different E_{up}. The anodic sweep is unaffected in all cases and the limiting current ascribed to OH^- oxidation is constant, irrespective of E_{up}; in contrast, the current recorded on the cathodic sweep decreases with increasing E_{up}, particularly so when E_{up} is well into the O_2 evolution region. These results confirm that the oxidation wave is sensitive to pH.

Since the oxide formation region is sensitive to pH, it should also be sensitive to the tip-substrate distance L, as a higher L should allow OH^- to diffuse away faster, thereby lowering its local concentration. Figure 7 shows the oxide formation region obtained with the waveform shown in Figure 5 for different L and with $t_{low} =$ 30 s; this time was selected to ensure that small quantities of OH^- were produced. The voltammograms show that the current for the early stage of oxide formation peak, circa 0.7 to 0.8 V, increases when decreasing L; we believe this occurs because the stronger the hindrance, the more alkaline is the solution trapped between the tip and the substrate, and the more oxide formation is promoted to lower potentials. In contrast, the second stage of oxide formation, circa 1.3 V, decreases when decreasing L, presumably because at shorter L, most of the oxide is formed at lower potentials due to the increasingly alkaline local solution. At very low

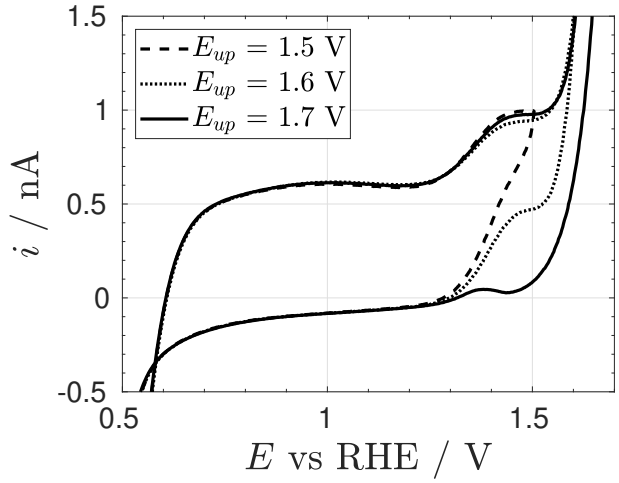

Figure 6: Same conditions as in Figure 5b: electrode in the hindered position, $t_{low} = 30$ s, $E_{low} = 0$ V and E_{up} was varied as indicated in the legend.

L, the local OH^- concentration is sufficiently high for the OH^- oxidation wave to appear. In the following section, we review the results and consider their implication for the voltammetry of Pt electrodes in presence of oxygen.

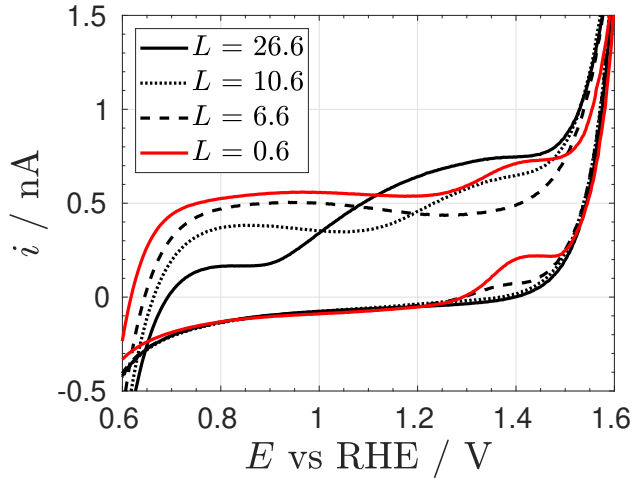

Figure 7: Cyclic voltammograms at 20 mV s^{-1} in Ar or O_2 saturated 0.1 M $KClO_4$ solution. The potential waveform shown in Figure 5a was used with $t_{low} = 30$ s and the tip-substrate distance was varied as indicated in the legend.

4 Discussion

All the results presented here lead us to conclude that the adsorbed species previously reported by our group are not due to the prior exposure of the Pt surface to dissolved oxygen but to local pH changes induced by the ORR. This is only observed in unbuffered neutral conditions because the high OH^- flux due to the ORR cannot be buffered by the solution. As the electrode environment becomes increasingly alkaline, the onset of oxide formation shifts to much lower potentials than predicted by the bulk pH. The pre-conditioning waveform used by Perry and Denuault [11, 12, 38] ensured that every experiment started with the same electrode history, but, because the waveform forced the electrode to be reduced in presence of oxygen, the local pH ended up being sufficiently alkaline to promote the formation of a low Pt oxide coverage at a much lower potential than anticipated. This oxide remained on the electrode, even after purging the solution with Ar, and its stripping during the subsequent potential step generated an extra current that was ascribed to an oxygenated adspecies. In future, the formation of the oxide could be avoided by selecting a lower rest potential but this would force the subsequent potential step to start from an initial condition where the ORR is already running. This compromise could be further improved by rapidly providing fresh solution with, for example, a wall jet arrangement.

The results reported here demonstrate that the common practice of subtracting the voltammogram recorded in absence of oxygen from that recorded in presence of oxygen is not appropriate when operating in unbuffered neutral conditions. They also demonstrate that the subtraction methodology is valid when the electrolyte is sufficiently acidic or alkaline to prevent changes in the local pH during the electrochemical reactions.

Pt oxide formation-reduction and Pt dissolution processes are interlinked in a complex manner [39] but the impact of dissolved oxygen on these processes is still poorly understood. Pt dissolution is generally associated with potentials above that of place exchange. In deaerated acidic conditions, place exchange was reported circa 1.15 $\pm$ 0.05 V [25] while in oxygenated acidic conditions, the dissolution of Pt was observed below 0.95 V, i.e. before the place exchange [10]. The results of Matsumoto and co-workers [10] are particularly interesting in the context of the present study. In their paper, figure 3 reveals that, in presence of oxygen, the amount of Pt detected in the H_2SO_4 solution significantly increased when the lower reversal potential of their cycles decreased below 0.8 V, i.e. when the lower limit of the cycles entered the ORR region. This therefore suggests that the ORR is having an impact on the Pt oxide electrochemistry, even in acidic conditions, but the effect is not trivial to observe. Matsumoto and co-workers reported the loss of 53 ng cm^{-2} of Pt after 4000 cycles, yet the CV recorded after 4000 cycles was identical to the initial one and the electroactive area was unchanged after 8000 cycles, figure 2b in their paper. On its own, the voltammetry presented here is not sufficient to locate the place exchange process nor is it capable of revealing at which potentials Pt dissolution occurs. Having clearly observed that the formation of Pt oxide occurs at lower potentials, we can only speculate that in neutral unbuffered conditions, the presence of oxygen promotes the place exchange process and the dissolution of Pt to lower potentials than predicted by the bulk pH. Our

experiments revealed significant alkalinisation of the local solution by the ORR because they were conducted in unbuffered neutral media. The results from Matsumoto and co-workers suggest that even in 0.5 M H_2SO_4, the ORR is capable of promoting Pt dissolution at potentials far below those expected from the bulk pH. It would be interesting to ascertain whether this also comes from some degree of local alkalinisation or from the ORR mechanism itself.

Conclusions

In unbuffered neutral aqueous media containing dissolved oxygen, the oxidation of Pt is significantly influenced by local changes of pH linked to the production of OH^- by the ORR. As the environment near the electrode becomes alkaline, the onset of oxide formation moves to potentials more negative than determined by the bulk pH and negative enough to overlap the onset of oxygen reduction. This occurs even with high rates of mass transfer. When the diffusion of OH^- away from the electrode is hindered, the hydroxide concentration builds up sufficiently to produce a new wave ascribed to the oxidation of OH^-. This study suggests that the oxide formed at potentials lower than predicted by the bulk pH is the oxygenated adspecies observed by Perry and Denuault [11, 12]. The potential window where they observed the adsorption, corresponds to the region where oxide forms because of the ORR. The results presented here provide convincing evidence that prior exposure of the Pt surface to dissolved oxygen does not promote the irreversible adsorption of oxygenated species and that it is not possible to obtain a Pt surface free from oxide at potentials positive of the onset of the ORR. These conclusions are consistent with the negligible effect of molecular oxygen on Pt oxide formation reported by the groups of Kongkanand and Liu [8, 9]. In acidic and basic solutions, the ORR is not able to alter the local pH appreciably and the voltammetry does not change as observed in unbuffered neutral conditions. Further investigations could include 1) repeating some of this work with buffers of increasing buffering capacity and 2) performing numerical simulations to assess quantitatively the changes in local pH in relation to the microelectrode voltammogram. Another important aspect of this study is the hindered diffusion methodology. It offers a number of advantages, in particular the ability to investigate the role of oxygen without having to degas or change the solution and the ability to decrease the rate of oxygen diffusion to a point where the voltammetry approaches that recorded in deaerated conditions. The methodology has revealed a lot more about the influence of the ORR on the Pt oxide region than could be gained from experiments in the bulk. The hindered diffusion concept is not restricted to the ORR and can also be used to discriminate the current contributions of surface bound and dissolved species.

5 Acknowledgements

O.R. thanks CONACYT-I2T2 for the scholarship provided (No. 411294) to pursue a PhD in Chemistry at the University of Southampton. The authors are grateful to the reviewers for their suggestions.

References

[1] I. Katsounaros, W. B. Schneider, J. C. Meier, U. Benedikt, P. U. Biedermann, A. A. Auer, K. J. J. Mayrhofer, Hydrogen peroxide electrochemistry on platinum: towards understanding the oxygen reduction reaction mechanism, Physical Chemistry Chemical Physics 14 (20) (2012) 7384.

[2] E. J. Coleman, A. C. Co, The complex inhibiting role of surface oxide in the oxygen reduction reaction, ACS Catalysis 5 (12) (2015) 7299–7311.

[3] Y.-J. Deng, M. Arenz, G. K. Wiberg, Equilibrium coverage of OH_{ad} in correlation with platinum catalyzed fuel cell reactions in $HClO_4$, Electrochemistry Communications 53 (2015) 41–44.

[4] R. Thacker, J. P. Hoare, Sorption of oxygen from solution by noble metals, Journal of Electroanalytical Chemistry and Interfacial Electrochemistry 30 (1) (1971) 1–14.

[5] J. P. Hoare, R. Thacker, C. R. Wiese, Sorption of oxygen from solution by noble metals: II. Nitric acid-passivated bright platinum, Journal of Electroanalytical Chemistry and Interfacial Electrochemistry 30 (1) (1971) 15–23.

[6] J. Drnec, M. Ruge, F. Reikowski, B. Rahn, F. Carlà, R. Felici, J. Stettner, O. M. Magnussen, D. A. Harrington, Pt oxide and oxygen reduction at Pt(111) studied by surface X-ray diffraction, Electrochemistry Communications 84 (2017) 50–52.

[7] A. A. Topalov, A. R. Zeradjanin, S. Cherevko, K. J. Mayrhofer, The impact of dissolved reactive gases on platinum dissolution in acidic media, Electrochemistry Communications 40 (2014) 49–53.

[8] A. Kongkanand, J. M. Ziegelbauer, Surface platinum electrooxidation in the presence of oxygen, The Journal of Physical Chemistry C 116 (5) (2012) 3684–3693.

[9] Y. Liu, M. Mathias, J. Zhang, Measurement of platinum oxide coverage in a proton exchange membrane fuel cell, Electrochemical and Solid-State Letters 13 (1) (2010) B1.

[10] M. Matsumoto, T. Miyazaki, H. Imai, Oxygen-enhanced dissolution of platinum in acidic electrochemical environments, The Journal of Physical Chemistry C 115 (22) (2011) 11163–11169.

[11] S. C. Perry, G. Denuault, Transient study of the oxygen reduction reaction on reduced Pt and Pt alloys microelectrodes: evidence for the reduction of pre-adsorbed oxygen species linked to dissolved oxygen, Physical Chemistry Chemical Physics 17 (44) (2015) 30005–30012.

[12] S. C. Perry, G. Denuault, The oxygen reduction reaction (ORR) on reduced metals: evidence for a unique relationship between the coverage of adsorbed oxygen species and adsorption energy, Physical Chemistry Chemical Physics 18 (15) (2016) 10218–10223.

[13] Y.-F. Yang, G. Denuault, Scanning electrochemical microscopy (SECM) : study of the adsorption and desorption of hydrogen on platinum electrodes in Na_2SO_4 solution (pH = 7), Journal of Electroanalytical Chemistry 418 (1-2) (1996) 99–107.

[14] Y.-F. Yang, G. Denuault, Scanning electrochemical microscopy (SECM): Study of the formation and reduction of oxides on platinum electrode surfaces in Na_2SO_4 solution (pH = 7), Journal of Electroanalytical Chemistry 443 (2) (1998) 273–282.

[15] M. Sosna, G. Denuault, R. W. Pascal, R. D. Prien, M. Mowlem, Development of a reliable microelectrode dissolved oxygen sensor, Sensors and Actuators B: Chemical 123 (1) (2007) 344–351.

[16] R. Shacham, D. Avnir, D. Mandler, Electrodeposition of methylated sol-gel films on conducting surfaces, Advanced Materials 11 (5) (1999) 384–388.

[17] I. Zhitomirsky, A. Petric, Cathodic electrodeposition of polymer films and organoceramic films, Materials Science and Engineering: B 78 (2-3) (2000) 125–130.

[18] H. Park, P. Ayala, M. A. Deshusses, A. Mulchandani, H. Choi, N. V. Myung, Electrodeposition of maghemite (γ-Fe_2o_3) nanoparticles, Chemical Engineering Journal 139 (1) (2008) 208–212.

[19] R. Schrebler, C. Llewelyn, F. Vera, P. Cury, E. Munoz, R. del Rio, H. G. Meier, R. Cordova, E. A. Dalchiele, An electrochemical deposition route for obtaining α-Fe_2O_3 thin films, Electrochemical and Solid-State Letters 10 (10) (2007) D95.

[20] C. Lefrou, R. Cornut, Analytical expressions for quantitative scanning electrochemical microscopy (SECM), ChemPhysChem 11 (3) (2010) 547–556.

[21] L. W. Liao, M. F. Li, J. Kang, D. Chen, Y.-X. Chen, S. Ye, Electrode reaction induced pH change at the Pt electrode/electrolyte interface and its impact on electrode processes, Journal of Electroanalytical Chemistry 688 (2013) 207–215.

[22] S. Strbac, The effect of pH on oxygen and hydrogen peroxide reduction on polycrystalline Pt electrode, Electrochimica Acta 56 (3) (2011) 1597–1604.

[23] M. Wakisaka, H. Suzuki, S. Mitsui, H. Uchida, M. Watanabe, Increased oxygen coverage at Pt-Fe alloy cathode for the enhanced oxygen reduction reaction studied by EC-XPS, The Journal of Physical Chemistry C 112 (7) (2008) 2750–2755.

[24] M. Wakisaka, H. Suzuki, S. Mitsui, H. Uchida, M. Watanabe, Identification and quantification of oxygen species adsorbed on Pt(111) single-crystal and polycrystalline Pt electrodes by photoelectron spectroscopy, Langmuir 25 (4) (2009) 1897–1900.

[25] G. Jerkiewicz, G. Vatankhah, J. Lessard, M. P. Soriaga, Y.-S. Park, Surface-oxide growth at platinum electrodes in aqueous H_2SO_4: Reexamination of its mechanism through combined cyclic-voltammetry, electrochemical quartz-crystal nanobalance, and Auger electron spectroscopy measurements, Electrochimica Acta 49 (9-10) (2004) 1451–1459.

[26] G. K. Wiberg, M. Arenz, Establishing the potential dependent equilibrium oxide coverage on platinum in alkaline solution and its influence on the oxygen reduction, Journal of Power Sources 217 (2012) 262–267.

[27] K. Aoki, K. Akimoto, K. Tokuda, H. Matsuda, J. Osteryoung, Linear sweep voltammetry at very small stationary disk electrodes, Journal of Electroanalytical Chemistry and Interfacial Electrochemistry 171 (1-2) (1984) 219–230.

[28] D. Pletcher, S. Sotiropoulos, Hydrogen adsorption–desorption and oxide formation–reduction on polycrystalline platinum in unbuffered aqueous solutions, J. Chem. Soc., Faraday Trans. 90 (24) (1994) 3663–3668.

[29] M. Alsabet, M. Grden, G. Jerkiewicz, Comprehensive study of the growth of thin oxide layers on Pt electrodes under well-defined temperature, potential, and time conditions, Journal of Electroanalytical Chemistry 589 (1) (2006) 120–127.

[30] W. Sheng, Z. Zhuang, M. Gao, J. Zheng, J. G. Chen, Y. Yan, Correlating hydrogen oxidation and evolution activity on platinum at different pH with measured hydrogen binding energy, Nature Communications 6 (1) (2015).

[31] C. Bragato, S. Daniele, M. A. Baldo, G. Denuault, Oxygen as redox mediator in scanning electrochemical microscopy. Application to the study of localised acid attack of marble., Annali di chimica 92 (2002) 153–161.

[32] A. J. Bard, G. Denuault, R. A. Friesner, B. C. Dornblaser, L. S. Tuckerman, Scanning electrochemical microscopy: theory and application of the transient (chronoamperometric) SECM response, Analytical Chemistry 63 (13) (1991) 1282–1288.

[33] J. L. Amphlett, G. Denuault, Scanning electrochemical microscopy (SECM): an investigation of the effects of tip geometry on amperometric tip response, The Journal of Physical Chemistry B 102 (49) (1998) 9946–9951.

[34] G. K. H. Wiberg, M. Arenz, On the influence of hydronium and hydroxide ion diffusion on the hydrogen and oxygen evolution reactions in aqueous media, Electrochimica Acta 158 (2015) 13–17.

[35] M. E. Abdelsalam, G. Denuault, M. A. Baldo, C. Bragato, S. Daniele, Detection of hydroxide ions in aqueous solutions by steady-state voltammetry, Electroanalysis 13 (4) (2001) 289–294.

[36] S. Daniele, M. A. Baldo, C. Bragato, G. Denuault, M. E. Abdelsalam, Steady-state voltammetry for hydroxide ion oxidation in aqueous solutions in the absence of and with varying concentrations of supporting electrolyte, Analytical Chemistry 71 (4) (1999) 811–818.

[37] S. Daniele, M. A. Baldo, C. Bragato, M. E. Abdelsalam, G. Denuault, Steady-state voltammetry of hydroxide ion oxidation in aqueous solutions containing ammonia, Analytical Chemistry 74 (14) (2002) 3290–3296.

[38] S. C. Perry, L. M. A. Shandoudi, G. Denuault, Sampled-current voltammetry at microdisk electrodes: Kinetic information from pseudo steady state voltammograms, Analytical Chemistry 86 (19) (2014) 9917–9923.

[39] P. P. Lopes, D. Tripkovic, P. F. Martins, D. Strmcnik, E. A. Ticianelli, V. R. Stamenkovic, N. M. Markovic, Dynamics of electrochemical Pt dissolution at atomic and molecular levels, Journal of Electroanalytical Chemistry 819 (2018) 123–129.